Simulation of Contactless Crack Detection in HTS Films: Application of *H*-Matrix Method to Fast Matrix-Vector Multiplication*)

Teruou TAKAYAMA, Ayumu SAITOH[1)], Atsushi KAMITANI[1)] and Hiroaki NAKAMURA[2)]

Department of Informatics, Yamagata University, Yonezawa 992-8510, Japan
[1)]*Graduate School of Science and Engineering, Yamagata University, Yonezawa 992-8510, Japan*
[2)]*National Institute for Fusion Science, Toki 509-5292, Japan*

(Received 30 November 2015 / Accepted 3 March 2016)

Detectability of the multiple cracks in a high-temperature superconducting (HTS) film by a scanning permanent magnet method has been investigated numerically. To this end, a numerical code has been developed for performing a shielding current analysis in an HTS film with cracks. Furthermore, the GMRES(k) method and the H-matrix method are adopted in the code. By using the code, the scanning permanent magnet method can be simulated successfully. The results of the computations show that the x-coordinate of the crack endpoint cannot be estimated with increasing the magnet radius. On the other hand, the y-coordinate of the crack endpoint can be detected accurately.

Keywords: crack detection, FEM, high-temperature superconductor, permanent magnet, simulation

DOI: 10.1585/pfr.11.2401043

1. Introduction

A superconductivity is a phenomenon characterized by the zero electrical resistance when materials are cooled to the critical temperature or less. As is well known, a high-temperature superconductors (HTSs) are used for developing various devices and systems such as nuclear fusion reactor, flywheel, MRI, and etc., and they are characterized by some parameters. In particular, a critical current density j_C is one of the most important parameters, and it is important to measure the value of j_C accurately.

As a contactless method and a high-speed method for measuring a critical current density j_C in an HTS film, Hattori *et al.* proposed the scanning permanent magnet method [1]. In the method, a permanent magnet is moved along a HTS surface. They found that a spatial distribution of j_C can be estimated from the distribution of an electromagnetic force acting on the film.

In order to simulate a scanning permanent magnet method, a numerical code was developed for analyzing the time evolution of a shielding current density in an HTS film with multiple cracks [2, 3]. After an initial-boundary-value problem of the shielding current density is spatially discretized with the finite element method (FEM), the resulting ordinary differential system is solved by using the backward Euler method and the Runge-Kutta (R-K) method with an adaptive step-size algorithm. In particular, it is found that the R-K method is a useful tool with increasing the number of nodes for the FEM. However, it is necessary to consider the further high-speed of the shielding current analysis for a large-scale problem.

The purpose of the present study is to investigate the detectability of the multiple cracks in the HTS film. In order to analyze a shielding current density, we apply the GMRES(k) method and H-matrix method to the linear systems obtained from the Backward Euler method.

2. Governing Equations

In a scanning permanent magnet method, a cylindrical magnet of radius R and height H is located just above an HTS thin film, and a distance between a magnet bottom and film surface is denoted by L. We assume a square-shaped HTS film of length a and thickness b, and the square cross-section of the film is denoted by Ω. If a crack is contained in the film, Ω has not only the outer boundary C_0 but the inner boundaries C_j ($j = 1, 2, \cdots, m$).

In the present study, we use the Cartesian coordinate system $\langle O : \boldsymbol{e}_x, \boldsymbol{e}_y, \boldsymbol{e}_z \rangle$, where the z-axis is parallel to the thickness direction and the origin O is the centroid of the film. In terms of the coordinate system, the symmetry axis of the coil is determined as $(x, y) = (x_M, y_M)$. For characterizing the magnet flux density at $(x, y, z) = (x_M, y_M, b/2)$ for $v = 0$ mm/s. The movement of the magnet is assumed as $x_M(t) = vt - a/2$, where v is the magnitude of the scanning velocity.

As is well known, a shielding current density $\boldsymbol{j}$ in an HTS is closely related to the electric field $\boldsymbol{E}$. The relation can be written as

author's e-mail: takayama@yz.yamagata-u.ac.jp
*) This article is based on the presentation at the 25th International Toki Conference (ITC25).

$$\boldsymbol{E} = E(|\boldsymbol{j}|)[\boldsymbol{j}/|\boldsymbol{j}|]. \tag{1}$$

As a function $E(j)$, we assume the power law

$$E(j) = E_{\mathrm{C}}[j/j_{\mathrm{C}}]^N, \tag{2}$$

where E_{C} is the critical electric field and N is a constant.

By using the thin-layer approximation [4, 5], the shielding current density $\boldsymbol{j}$ can be expressed as

$$\boldsymbol{j} = (2/b)\nabla S \times \boldsymbol{e}_z, \tag{3}$$

and the time evolution of the scalar function $S(\boldsymbol{x}, t)$ is governed by the following integro-differential equation:

$$\mu_0 \partial_t(\hat{W}S) + (\nabla \times \boldsymbol{E}) \cdot \boldsymbol{e}_z = -\partial_t \langle \boldsymbol{B} \cdot \boldsymbol{e}_z \rangle, \tag{4}$$

where a bracket $\langle\ \rangle$ is an average operator over the thickness of the HTS film. Also, $\hat{W}$ is defined by

$$\hat{W}S = \iint_{\Omega} Q(|\boldsymbol{x} - \boldsymbol{x}'|)S(\boldsymbol{x}', t)\mathrm{d}^2\boldsymbol{x}' + (2/b)S(\boldsymbol{x}, t), \tag{5}$$

and an explicit function $Q(r)$ in (5) is expressed as follows:

$$Q(r) = -(\pi b^2)^{-1}[r^{-1} - (r^2 + b^2)^{-1/2}]. \tag{6}$$

The initial and boundary conditions to (4) are assumed as follows:

$$S = 0, \quad \text{on} \quad C_0 \tag{7}$$

$$\frac{\partial S}{\partial s} = 0, \quad \text{on} \quad C_i \tag{8}$$

$$h(\boldsymbol{E}) \equiv \oint_{C_i} \boldsymbol{E} \cdot \boldsymbol{t}\mathrm{d}t = 0. \tag{9}$$

Here, s and $\boldsymbol{n}$ are an arclength along C_i and a normal unit vector on C_i, respectively.

3. Numerical Methods

3.1 Discretization

In the present study, we discretize the initial-boundary-value problem of (4) in time and space using the finite element method (FEM) and the Backward Euler method, respectively. A region Ω is divided into a number N_{e} of square elements. On the other hand, a crack is given by a line segment.

By using the Backward Euler method, the initial-boundary-value problem of (4) is transformed into the nonlinear boundary-value problem as follows:

$$(*1)\begin{cases} G(S^{(n+1)}) = 0, & \text{in} \quad \Omega & \text{(10a)} \\ S^{(n+1)} = 0, & \text{on} \quad C_0 & \text{(10b)} \\ \partial S^{(n+1)}/\partial s = 0, & \text{on} \quad C_i & \text{(10c)} \\ \oint_{C_i} \boldsymbol{E}^{(n+1)} \cdot \boldsymbol{t}\mathrm{d}s = \phi_i, & & \text{(10d)} \\ N(\boldsymbol{E}^{(n+1)}) = 0. & & \text{(10e)} \end{cases}$$

Here, a superscript (n) is a value at time $t = t^n(\equiv n\Delta t)$. In addition, $G(\boldsymbol{S}^{(n+1)})$ is defined by

$$G(S^{(n+1)}) \equiv \mu_0 \hat{W} S^{(n+1)} + \Delta(\nabla \times \boldsymbol{E}^{(n+1)}) \cdot \boldsymbol{e}_z - u, \tag{11}$$

where u is

$$u = \mu_0 \hat{W} S^{(n)} - (\langle \boldsymbol{B}^{(n+1)} \cdot \boldsymbol{e}_z \rangle - \langle \boldsymbol{B}^{(n)} \cdot \boldsymbol{e}_z \rangle). \tag{12}$$

Note that numerical solution contains the error due to which a boundary condition (9) is not satisfied. In order to resolve this problem, we propose the virtual voltage method [5]. In the method, we use a numerical boundary condition (10e), where $N(\boldsymbol{E})$ is evaluated from $h(\boldsymbol{E})$. Therefore, the solution of the problem (*1) include not only $S^{(n+1)}$ but also ϕ_i.

When the FEM and the Newton method are applied to the problem (*1), we get simultaneous equations system:

$$\begin{bmatrix} A(\boldsymbol{S}) & C & F(\boldsymbol{\phi}) \\ C^T & O & O \\ D^T(\boldsymbol{S}) & O & O \end{bmatrix} \begin{bmatrix} \delta\boldsymbol{S} \\ \boldsymbol{\lambda} \\ \delta\boldsymbol{\phi} \end{bmatrix} = \begin{bmatrix} \boldsymbol{g}(\boldsymbol{S}, \boldsymbol{\phi}) \\ \boldsymbol{0} \\ -\boldsymbol{h}^*(\boldsymbol{S}) \end{bmatrix}, \tag{13}$$

at each time step of the Newton method. Here, $\boldsymbol{S}$ is the n-vector, and the n is a number of nodes for the FEM. The $(m-n)$-by-n matrices $A(\boldsymbol{S})(\equiv W + J(\boldsymbol{S}))$ is determined from $\hat{W}$, where $J(\boldsymbol{S})$ is the Jacobian matrix. The matrix C, $F(\phi)$, $D(\boldsymbol{S})$, and the vector $\boldsymbol{g}(\boldsymbol{S}, \phi)$ are obtained by the cracks. As a result, the initial-boundary problem of (4) is reduced to the simultaneous equations system at each time step of the Newton method. The procedure for the system is as follows:

1. By solving the simultaneous equations, we get the correction $\delta\boldsymbol{S}$ and $\delta\boldsymbol{\phi}$.
2. We update an approximate solutions by means of $\boldsymbol{S}^{(j)} \Leftarrow \boldsymbol{S}^{(j-1)} + \delta\boldsymbol{S}$ and $\boldsymbol{\phi}^{(j)} \Leftarrow \boldsymbol{\phi}^{(j-1)} + \delta\boldsymbol{\phi}$.

Two procedures are repeated until the termination condition:

$$\max(\|\delta\boldsymbol{S}\|/\|\boldsymbol{S}\|, \|\delta\boldsymbol{\phi}\|/\|\boldsymbol{\phi}\|) \leq \varepsilon, \tag{14}$$

is satisfied. Here, ε is a constant, and $\|\ \ \|$ denotes the maximum norm. Under the numerical method, we develop the numerical code for analyzing the time evolution of the shielding current density in an HTS film with multiple cracks.

3.2 High-speed method for shielding current analysis

In this subsection, we propose a high-speed analysis of a shielding current density in an HTS film. To this end, we use the GMRES(k) method as a solver of simultaneous equations (13), and we measure the CPU time for the simulation of a scanning permanent magnet method Here, a convergence criterion of the GMRES(k) method is denoted by ε_{G}.

As is well known, a matrix-vector product is calculated at the each iteration in the GMRES(k) method. In order to calculate the matrix-vector product with a further high-speed, we apply the H-matrix method [6] with the adaptive cross approximation [7–9] to the matrix W. In the H-matrix method, the computation of the matrix-vector product can be reduced by compressing the matrix.

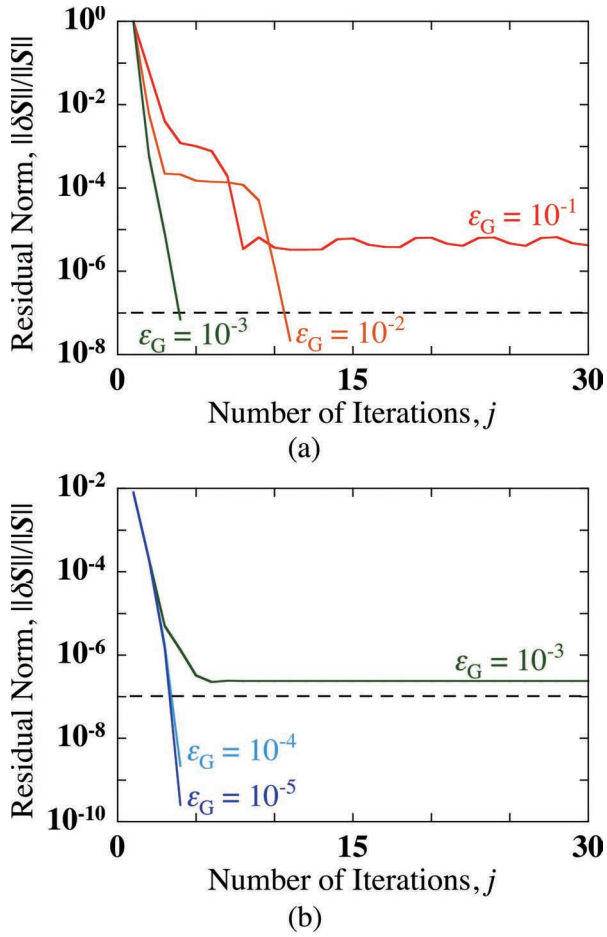

Fig. 1 Residual history of the Newton method for the case with (a) $x_M = -9.9$ mm and (b) $x_M = -4.3$ mm. Here, $k = 500$ and $n = 2601$.

Throughout the present study, the physical and geometrical parameters are fixed as follows: $a = 20$ mm, $b = 1$ μm, $j_C = 2$ MA/cm^2, $E_C = 1$ mV/m, $N = 20$, $L = 0.5$ mm, $H = 2$ mm, $B_F = 0.3$ T, $v = 10$ cm/s, and $\varepsilon = 10^{-7}$. In addition, we suppose the two cracks, C_1 and C_2, are included in the HTS film, and its shape is a line segment which is parallel to the x-axis. The crack distance d and the crack size L_c are given by $d = 4$ mm and $L_c = 1.6$ mm.

Firstly, we investigate the influence of the Newton method on the convergence determinant of GMRES(k) method. In Figs. 1, we show the residual history of the Newton method. We see from Fig. 1 (a) that, for $\varepsilon_G = 10^{-1}$, the value of the residual norm almost becomes constant, whereas the Newton method converges in 11 and 4 iterations for $\varepsilon_G = 10^{-2}$ and $\varepsilon_G = 10^{-3}$, respectively. On the other hand, we cannot obtain the solution at this step for $\varepsilon_G = 10^{-3}$ (see Fig. 1 (b)). In addition, for $\varepsilon_G = 10^{-4}$ and $\varepsilon_G = 10^{-5}$, the Newton method converges in 4 iterations. Consequently, it is necessary that the convergence determinant is $\varepsilon_G \leq 10^{-4}$. In the following, the value of ε_G is fixed to $\varepsilon_G = 10^{-5}$.

Next, we investigate the influence of the restart coefficient k on the CPU time. In Fig. 2, we show the dependence

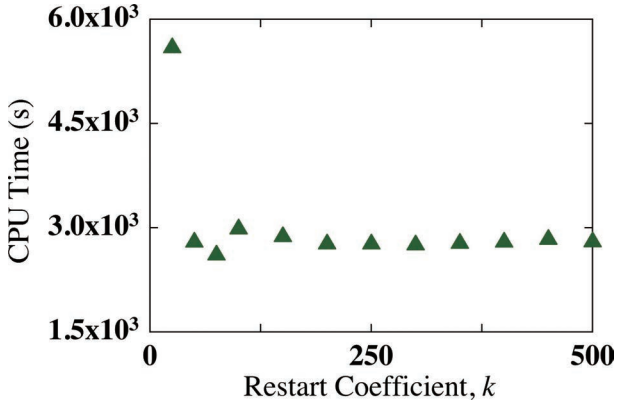

Fig. 2 Dependence of the CPU time on the restart coefficient k for the case with $n = 2601$.

of the CPU time on the restart coefficient k. From this figure, the CPU time decreases with increasing the value of k monotonously for $25 \leq k \leq 75$, and it almost becomes a constant. Especially, the CPU time drastically increases for $k = 25$. As a result, it is found that the CPU time decreases by using the large value of k. Hereafter, we use $k = 500$ as the the value of the restart coefficient for analyzing the shielding current density.

We found that, by using the GMRES(k) method to as a linear-system solver, the time evolution of the shielding current can be analyzed with high speed. In addition, the speed of the GMRES(k) method can be accelerated by using the H-matrix method.

4. Detectability of Multiple Cracks

In this section, we numerically investigate the detectability of the multiple cracks by the scanning permanent magnet method. For this purpose, we adopt a defect parameter d_s [5] as usual. By using the defect parameter, a relatively value can be obtained near the cracks, and its value almost vanishes around the film edge.

Firstly, we investigate the distribution of the defect parameter d_s. In Figs. 3, we show the contour maps of the defect parameter d_s for the two types of the magnet radius R. From Fig. 3 (a), d_s has a small value on both sides of the two cracks, whereas the maximum value of d_s is taken near the center of the HTS film. Figure 3 (b) indicates that we obtain a region of the small value by using the small radius. These results mean the crack position can be estimated from the smallest value of the defect parameter d_s. In Figs. 3, we also show the smallest value of d_s by a rhombus symbol in the first quadrant. Hereafter, the xy-coordinates of this symbol are denoted by $(x, y) = (x_s, y_s)$. The results of the computations show that we get $(x_s, y_s) = (2.3$ mm, 2 mm) and $(x_s, y_s) = 0.67$ mm, 2 mm for the case with $R = 3$ mm and $R = 0.5$ mm, respectively.

Next, let us investigate the detect accuracy of the multiple cracks numerically. To this end, as a measure of the accuracy, we define relative errors: $e_x \equiv |x_c^* - x_s|/x_c^*$ and

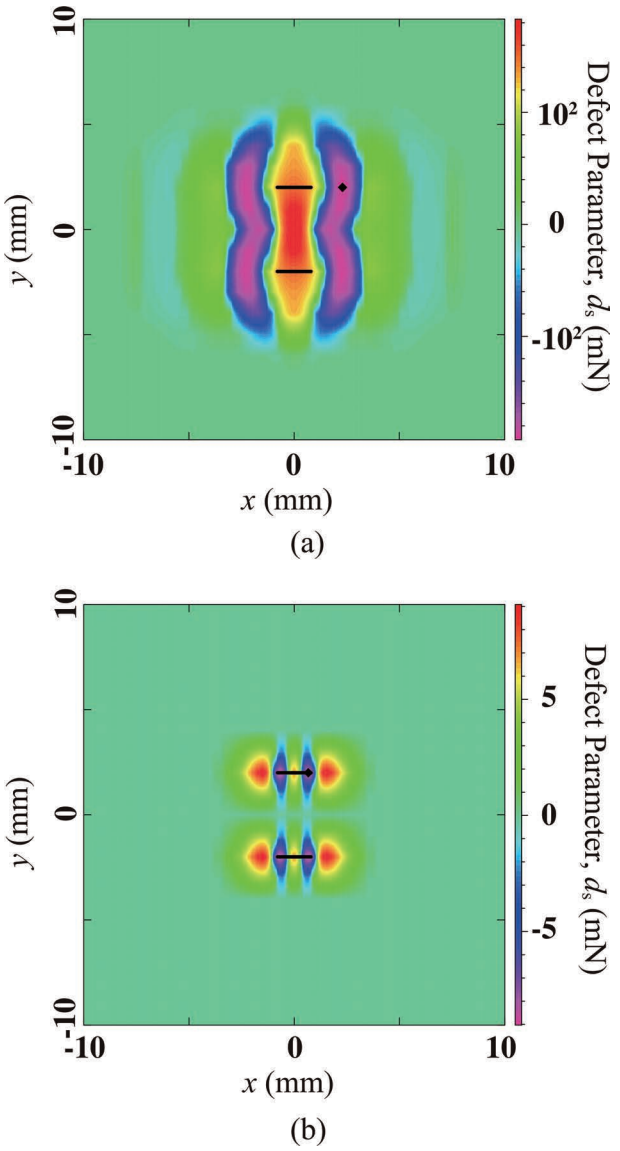

Fig. 3 Contour maps of the defect parameter d_s for (a) $R = 3$ mm and (b) $R = 0.5$ mm.

$e_y \equiv |y_c - y_s|/y_c$, where x_c^* is defined by $x_c^* \equiv L_c/2$. The relative error ε_x is calculated as a function of the magnet radius R and is depicted in Fig. 4. We see from this figure that the relative error e_x decreases with R for $R \leq 1$ mm, and its value monotonously increases with R for $R \geq 1$ mm. On the other hand, the value of e_y becomes $e_y = 0\%$ for 0.5 mm $\leq R \leq 3$ mm, and the y-coordinate of the crack position can be detected with a high accuracy.

5. Conclusion

Conclusions obtained in the present study are summarized as follows:

1. The Newton method does not converge at a certain time step when the convergence determinant of the GMRES(k) method is greatly larger than that of the Newton method. Also, we found the CPU time decreases by the large value of the restart coefficient k.
2. The x-coordinate of the crack endpoint cannot be fairly evaluated with increasing the magnet radius. On the other hand, the y-coordinate of the crack endpoint can be detected accurately.

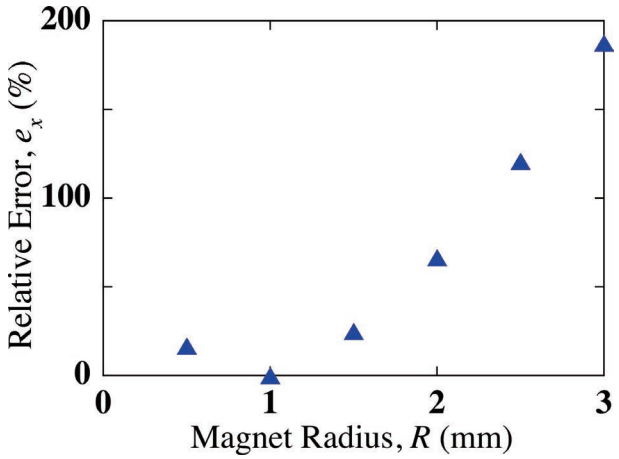

Fig. 4 Dependence of the relative error e_x on the magnet radius R.

In the future, we plan to compare the numerical results and the experimental ones next year.

Acknowledgment

This work was supported in part by Japan Society for the Promotion of Science under a Grant-in-Aid for Scientific Research (C) (No. 26520204 and No. 15K05926) A part of this work was also carried out with the support and under the auspices of the NIFS Collaboration Research program (NIFS15KNTS041, NIFS15KNXN297). Moreover, the numerical computations were carried out on Fujitsu PRIMEHPC FX100 of the LHD Numerical Analysis Server in NIFS.

[1] K. Hattori, A. Saito, Y. Takano, T. Suzuki, H. Yamada, T. Takayama, A. Kamitani and S. Ohshima, Physica C. **471**, 1033 (2011).
[2] T. Takayama and A. Kamitani, IEEE Trans. Appl. Supercond. **23**, 9001107 (2013).
[3] T. Takayama and A. Kamitani, IEEE Trans. Appl. Supercond. **24**, 9001505 (2014).
[4] A. Kamitani and S. Ohshima, IEICE Trans. Electron. **E82-C**, 766 (1999).
[5] A. Kamitani, T. Takayama and S. Ikuno, Physica C. **494**, 168 (2013).
[6] M. Bebendorf, Numer. Math. **86**, 565 (2000).
[7] S. Kurz, O. Rain and S. Rjasanow, IEEE Trans. Magn. **38**, 421 (2002).
[8] Y. Takahashi, C. Matsumoto and S. Wakao, IEEE Trans. Magn. **43**, 1277 (2007).
[9] V. Le-Van, B. Bannwarth, A. Carpentier. O, Chadebec. J. M. Guichon and G. Meunier, IEEE Trans. Magn. **50**, 7010904 (2014).